

Dental Apical Inflammation Score (DAIS): Histopathological scoring for the evaluation of the apical inflammatory activity and local bone destruction

S. Krenn^{a,*}, R. Gutwald^a, M. Bönigk^c, V. Krenn^b

^a Danube Private University, Krems-Stein, Austria

^b MVZ-Zentrum für Histologie, Zytologie und Molekulare Diagnostik, Trier, GmbH, Germany

^c Universität Wien, Vienna, Austria

ARTICLE INFO

Keywords:

Histopathology
Apical periodontitis
Radicular cysts
Dental Apical Inflammation Score (DAIS)
Osteitis

ABSTRACT

Objective: The purpose of this study was to evaluate 210 periapical lesions with a newly created Dental Apical Inflammation Score/DAIS with regard to their inflammatory cell infiltration, bone tissue, epithelium, bacteria and foreign material.

Study design: Specimens were obtained from 51 different dental practices over a period of 11 months. These specimens were then sent in for histopathological routine diagnostics.

Results: The DAIS classified 81 cases of Type 1 (acute inflammation = low, chronic inflammation = low), 79 cases of Type 2 (acute inflammation = low, chronic inflammation = high), 46 cases of Type 3 (acute inflammation = high, chronic inflammation = low) and 4 cases of Type 4 (acute inflammation = high, chronic inflammation = high). Bone tissue was found in 141 cases, signs for bacterial osteitis in 49 cases, cyst epithelium in 40 cases and foreign material in 27 cases. In 210 cases, cyst epithelium was evident in 27.2 % of Type 1, 15.2 % of Type 2, 8.7 % of Type 3 and in 50 % of Type 4 ($p = .019$). The 141 cases containing bone tissue showed signs of bacterial osteitis in 16.1 % of Type 1, 29.8 % of Type 2, 77.8 % of Type 3 and in 100 % of Type 4 ($p < .001$). In 64 cases, Bacteria was evident in 30 % of Type 1, 25 % of Type 2, 55 % of Type 3 and in 100 % of Type 4 ($p = .013$).

Conclusion: The DAIS could classify apical lesions with statistically significant differences. Bacterial osteitis in apical lesions was reported for the first time.

1. Introduction

Bacterial infection and necrosis of the dental pulp can lead to apical periodontitis, which may result in an apical granuloma or an apical cyst [1]. Treatment is carried out through effective root canal treatment in which the infected parts of the pulp are removed [2]. If however the apical lesion remains, the root canal treatment is reviewed, or a root tip resection is conducted as an apical surgical measure to prevent further bacterial contamination of the root canal system into the periradicular tissue [3]. Apical lesions contain various populations of acutely inflammatory and chronically inflammatory cells [4,5]. Histologically, they are characterised by fibrous connective and granulation tissue, proliferating epithelium and various inflammatory cell types [6,7]. The dominant cell types are lymphocytes, plasma cells, macrophages and neutrophils [8]. Radicular granulomas represent an initial reparative process of the local inflammation, whereas a proliferation of the epithelial cell rests of Malassez may lead to epithelial islands or a

radicular cyst [9,10]. Within apical lesions, the incidence of apical cysts is given as 6–55 % [11]. Regarding the pathogenesis, it is clear that the humoral and cellular immune systems play an important role. Factors like prostaglandin, interleukin, proteases, and proinflammatory cytokines such as TNF-alpha, IL-1 and IL-6, which are secreted by inflammatory and mesenchymal stem cells in the cyst, can lead to skeletal homeostasis in the form of osteoclast formation or bone resorption [5, 12]. Bacterial endotoxins also play a role in cyst growth and bone destruction [13]. There is no scientific consensus regarding the presence of bacteria in cysts. Although cyst fluids have been investigated for bacteria, in some studies no bacteria could be found [13]. In other research, however, bacteria were found in the cyst fluid or in the cysts themselves [14,15]. Regardless of the different causal pathogenesis, apical lesions have an inflammatory infiltration with local tissue destruction. Although the histopathological assessment of apical granuloma and radicular cysts is a widespread routine diagnostic procedure, there is as yet no standardised diagnostic assessment procedure in the

* Corresponding author at: Danube Private University, Krems-Stein, Austria.
E-mail address: h.simonkrenn@gmail.com (S. Krenn).

<https://doi.org/10.1016/j.prp.2020.153223>

Received 5 June 2020; Received in revised form 11 September 2020; Accepted 12 September 2020

Available online 21 September 2020

0344-0338/© 2020 Elsevier GmbH. All rights reserved.

form of a score to assess these inflammatory infiltrations. Histopathological scores, being defined assessment methods, are generally of great significance for the diagnosis of inflammatory and infectious diseases, and they are also included in international diagnostic guidelines for oral pathology [16]. One of the authors of the present paper (K.V) has participated in the interdisciplinary development of histopathological scores for inflammation pathology over the past 15–20 years, for example the Synovialitis Score [17], the Consensus Classification of peri-implant synovitis [18,19], the Histopathological Osteomyelitis Evaluation supported Score HOES [20], the CD15 focus score [21,22], and the Particle Algorithm for Foreign Material Deposits [23], which were well received internationally and are recognised as diagnostic standards in histopathological diagnosis [24]. The HOES was used in this work in order to analyse bone fragments for signs of bacterial infection. Tiemann et al. have shown that the HOES had a correlation of 68 % between preoperative diagnosis and histological analysis [20]. The reproducibility and applicability of the HOES score to osteomyelitis was and clinically confirmed by Stupina et al. [25].

2. Objective and score structure

A semi-quantitative, staged histopathological score with dual assessment mode, the Dental Apical Inflammation Score (DAIS), was developed that classifies inflammatory infiltration and has the following characteristics:

- 1 Semi-quantification (low grade versus high grade) of acute granulocyte-rich (acute) and chronic mononuclear inflammatory infiltration (chronic).
- 2 Assessment of the bone tissue and specification of osteitis using the Histopathological Osteomyelitis Evaluation Score (HOES) of Tiemann et al. 2014 [20].
- 3 Detection and characterisation of foreign material deposits.
- 4 Cyst epithelium detection

3. Patients and methods

3.1. Patients

All study procedures followed the tenets of the Declaration of Helsinki. The patients' age (female = 95, male = 115) had an arithmetic mean of 50.6 years (standard deviation: 16.7). The study was carried out in accordance with the ethical guidelines and regulations and had been approved by the Ethics Committee of the Medical Association of Rhineland-Palatinate; Mainz, Germany [Case Number: 2019-14637].

3.2. Clinical data

During the time from January to November 2019, 210 human tissue samples of apical lesions of three different German federal states from 57 different medical dental practices had been analysed. All tissue samples were taken from patients undergoing therapeutic interventions and the resected tissues had been submitted for histopathologic routine diagnostics. The clinical investigations included the issue of a radicular cyst in 173 cases, apical granuloma or apical periodontitis in 22 cases, and in 15 cases there was no specific issue. Data regarding possible dental pretreatments were not available.

3.3. Histopathological processing of the tissue samples

The macroscopic gross examination, tissue sampling, the processing of the samples including tissue sample paraffin-processing, decalcifying procedures, histochemical methods, and diagnostic histopathological classification had been performed in automatic and semi-automatic systems under a certified and accredited framework (quality standard according to DIN: DIN EN ISO/IEC 17020:2012, registry number: D-IS-

21311-01-00).

3.4. Gross examination of tissue samples

Soft tissue and osseous tissue: after fixing in buffered formalin (4%) for at least 24 h, tissue samples with a size up to 20 × 120 × 10 mm where completely embedded. In cases of tooth adhering cysts, bone tissue or soft tissue or the adhering soft tissue was removed; tooth tissue itself was not further processed but described and documented.

3.5. Decalcification

The decalcification was carried out by means of acid (7,5 % hydrochloric acid). The ratio of decalcification liquid volume to tissue sample volume was about 1:20. The reaction temperature was room temperature over an incubation time of about 1–3 h. The consistency of the samples had been checked after 1–3 h in order to prove the applicability for further cutting procedures in the microtome.

3.6. Histopathology and tissue staining

The microtomed tissue sections (two microtomed sections per case) with a section thickness of 1–3 µm were stained with haematoxylin and eosin (HE) staining, modified Giemsa staining and Grocott staining in a fully automated system (Leica- PELORIS® or SACURA-VIP-6 -AI®) with a barcode-tracking system (Roche, VANTAGE workflow solution®). These systems are closed and pressure / vacuum-based systems with very low emissions thereby ensuring especially high-quality results and high consistency as well reproducibility of the staining results. Oil Red O staining and Gram staining were performed manually by hand. This special staining had been carried out after evaluating the HE stained slides, especially in cases with bacterial colonisation and in cases with material deposits, thereby defining bacterial infections and material deposits.

4. Structure of the Dental Apical Inflammation Score

4.1. General scoring principles

For the detection of score features in the conventionally stained HE slides, objective magnification of 20 x (area size about: 1.3 qmm) and 40 x (area size about: 0.65 qmm) were used. Polarisation analysis was used for the typing of bone tissue (lamellar and non-lamellar bone) and for particle definition. The histopathological diagnosis and further evaluation were carried out by a pathologist specialising in inflammatory pathology (KV) and was independently verified by a student of dental medicine who holds a bachelor's degree in biotechnology (KS).

5. DAIS scoring definitions and DAIS score structure

5.1. Quantitative definition: confluent (high) versus non-confluent (low) pattern

In the overview enlargement (HE staining, final magnification around 100 x), a dual assessment was made to determine whether a confluent, dense infiltration pattern (high grade) or a non-confluent, non-dense infiltration pattern (low grade) was present. Confluent means that the leukocytes are arranged closely side by side (Fig. 1a). Non-confluent means that the leukocytes are not arranged side-by-side but are separated by connective tissue (Fig. 1b-d).

5.2. Qualitative definitions: acute and chronic inflammation

The characterisation of the infiltrate cells was likewise conducted with a dual categorisation format with a stronger magnification (final magnification around 400 x). "Acute inflammation" was defined by

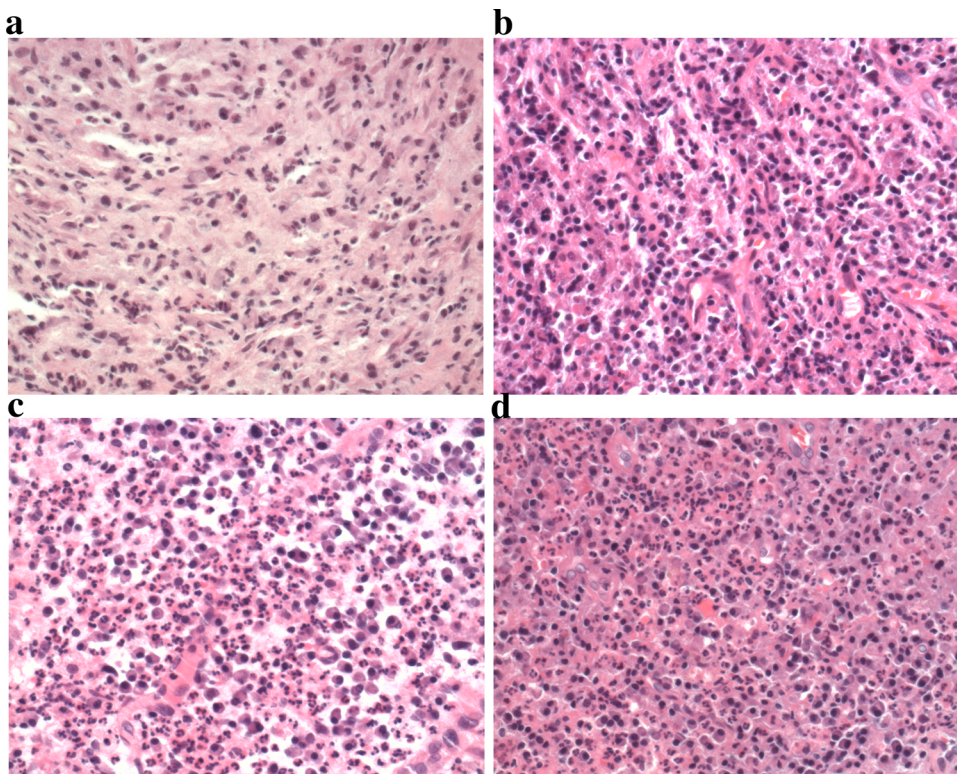


Fig. 1. Representation of the DAIS Types 1 to 4.

A, DAIS 1 (acute inflammation = low, chronic inflammation = low). **B**, DAIS 2 (acute inflammation = low, chronic inflammation = high). **C**, DAIS 3 (acute inflammation = high, chronic inflammation = low). **D**, DAIS 4 (acute inflammation = high, chronic inflammation = high). The lowest infiltrate density is found with DAIS 1 (**A**) the greatest infiltrate density is found with DAIS 4 (**D**) (HE staining, original magnification: around 400 x).

segmented neutrophils. “Chronic inflammation” was characterised by a mononuclear cell population consisting of lymphocytes, macrophages, histiocytes and plasma cells. The standard HE staining enables this discrimination, and so no further special stains were necessary.

6. DAIS types (DAIS 1 to DAIS 4)

4 combinations of tissue with inflammation infiltration were defined according to infiltrate quality and infiltrate quantity. DAIS 1 (acute inflammation = low, chronic inflammation = low), DAIS 2 (acute inflammation = low, chronic inflammation = high), DAIS 3 (acute inflammation = high, chronic inflammation = low) and DAIS 4 (acute inflammation = high, chronic inflammation = high). These different DAIS Types 1–4 are presented in Fig. 1a-d; the minimum infiltration density of the infiltration pattern was evident for DAIS 1 (Fig. 1a) and the maximum infiltration density for DAIS 4 (Fig. 1d)

6.1. Histopathological bacteria detection

The detection of bacteria was carried out at a final magnification of around 200 x to 400 x with HE staining, modified Giemsa staining, Gram staining and Grocott staining. The types included cocci, bacilli, vibrio and spirilla. These bacteria were arranged in variably large bacterial intra- and extra-cytoplasmic aggregates as well as in colonies (e.g.: *Actinomyces israelii*). The assessment did not distinguish between these bacterial arrangements.

6.2. Bacteria localisation in relation to different tissue types

The relation of the bacteria to tissue components was analysed. This included the relation of the bacteria to fibrous tissue, necrotic tissue as well as bone tissue with inflammatory infiltration. Epithelial components were not considered. 20 cases selected at random from the collective of all DAIS types (DAIS 1, 2, 3 and 4) were analysed; only 4 cases were available for DAIS 4. 12 cases with granulocyte-rich osteitis were additionally analysed for bacterial colonisation of bone fragments.

6.3. Osteitis definition

The evaluation of osteitis had been carried out according to the HOES. The HOES is a descriptive evaluation which provides information with respect to a bacterial infection and its activity in the bone tissue. The HOES was initially developed for skeletal bone tissue and was adapted for peri-apical bone tissue [20].

6.4. Particle material characterisation

The descriptive particle characterisation followed the particle algorithm of Krenn et al. that was developed for endoprosthesis materials and particle deposits in joint diseases and is used in routine diagnostic procedures. [23,26]. This principle was transferred to the peri-apical tissue. All particle categories were consequently described according to their size, shape, colour, and properties observed with conventional light microscopy with or without polarised light and by means of Oil Red O staining. The particle size ranges were determined using computer-aided interactive morphometric analysis, Leica DM 2005, microsystems framework 2007 using a similar computer-aided system, Zeiss Axioskop 40, Jenoptik ProgRes microscope camera. The systems were calibrated using a standard micrometre glass slide with 1 mm horizontal scale, 100 divisions – 10 μ m intervals (Perino et al. 2017).

7. Statistical analysis

The distribution of the epithelisation between the four independent DIAS groups was examined by using the Chi-squared test. Fisher’s exact test (two-tailed) was conducted due to the small sample size in group DAIS 4. Analyses were identical for bone fragments. Effect sizes were reported as Cramers V. As the data did not meet the criteria for an analysis of variance (ANOVA), a Kruskal-Wallis test was performed to examine the difference in sample size and the age of the patients across the four DAIS groups. An alpha level of $\alpha = 0.05$ was used for all tests of statistical significance. All data were processed using statistical analysis software (IMB SPSS-Statistics 22).

8. Results

8.1. Patients

210 tissue samples of apical lesions from 115 male and 95 female patients were analysed; these originated from 51 dental clinics in the federal states of Lower Saxony, Saarland and Rhineland-Palatinate. The arithmetic mean of the patients' ages was 50.6 years (standard deviation: 16.7). 122 (58 %) of the samples were from the upper jaw, 88 (42 %) from the lower jaw. In all cases, only various inflammation processes, but no malignant tumours, were diagnosed. The distribution of the sample size of the patients within the DAIS types was determined using the Kruskal-Wallis test. A Kruskal-Wallis test showed no statistically significant difference between the four DAIS groups ($\chi^2(3) = 5.382$, $p = .146$). The distribution of the patients' ages within the DAIS types was examined by means of the Kruskal-Wallis test. A Kruskal-Wallis test showed no statistically significant difference between the four DAIS groups ($\chi^2(3) = 3.414$, $p = .332$).

8.2. DAIS

After assessment by means of the DAIS score, 81 (38.6 %) cases were classified as Type 1, 79 (37.6 %) cases as Type 2, 46 (21.9 %) cases as Type 3 and 4 (1.9 %) cases as Type 4 (Figs. 1 and 2). No cases were observed that presented no inflammatory infiltration, exclusively low chronic inflammation, or exclusively low acute inflammation.

8.3. Epithelium detection

Of the 210 samples, epithelium was diagnosed in 40 cases (19 %). Epithelium was observed in 27.2 % of Class 1, 15.2 % of Class 2, 8.7 % of Class 3 and 50 % of Class 4. $\chi^2(3) = 9,799$, $p = .016$, $V = .217$ Fisher's exact test. The distribution was significant, with a small to medium effect size.

8.4. Bone components and bacterial osteitis

According to the HOES classification, it was possible to distinguish between bone tissue with signs of a bacterial infection and bone tissue with signs of chronic, exclusively inflammatory bone remodelling (new formation of woven bone). Of the 210 samples, bone particles were observed in 141 cases (67.1 %), and 48 samples (22.9 %) presented histopathological indications of bacterial osteitis. Of the 141 samples that contained bone, indications of bacterial osteitis were found in 16.1 % of Type 1, 29.8 % of Type 2, 77.8 % of Type 3 and 100 % of Type 4.

$\chi^2(3) = 32,273$, $p < .001$, $V = .487$ Fisher's exact test. The distribution was significant, with a medium to large effect size. The distribution of bone fragments among the DAIS types was almost random.

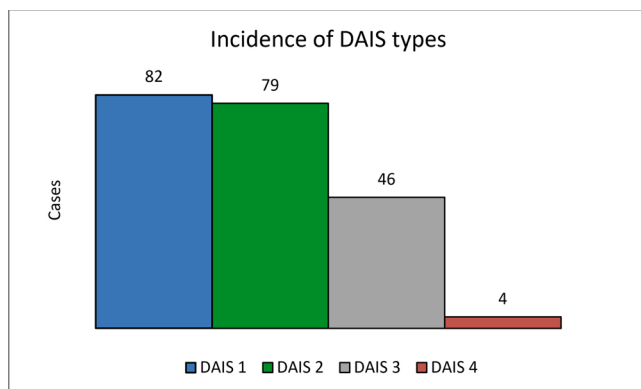


Fig. 2. Quantitative distribution of DAIS Types 1 to 4 in the investigated collective (n = 210).

8.5. Bacteria detection

For DAIS 1, bacteria were detected in 6 of 20 cases (30 %), for DAIS 2 in 5 of 20 cases (25 %), for DAIS 3 in 11 of 20 cases (55 %) and for DAIS 4 in 4 of 4 cases (100 %). $\chi^2(3) = 9,924$, $p = .013$, $V = .405$ Fisher's exact test. The distribution was significant, with a medium to large effect size. The bacterial detection contained extracellular bacterial aggregates, bacteria colonies (Fig. 3a), as well as intracellular/intracytoplasmic localised bacteria in segmented neutrophils and macrophages (Figs. 3b and 4 b). The bacteria colonies and *Actinomyces israelii* (Fig. 3c) were deposited on the tissue with the inflammation infiltration.

8.6. Bacteria localisation for different tissue types

All detected forms, intracellular/intracytoplasmic localisation in segmented neutrophils and macrophages, and extracellular bacterial aggregates in the form of so-called bacteria colonies were partly observed on necrotic tissue sections and also on tissue with inflammatory infiltration in DAIS 1 to DAIS 4 (Figs. 3a, b, 4 b). It was not possible to differentiate unambiguously between natural tissue surface and tissue fragmentation resulting from removal. 12 cases with pronounced granulocyte-rich osteomyelitis (Fig. 4a) were analysed. In 4 cases, bacteria were found in segmented neutrophils and macrophages on the cancellous bone (Fig. 4b).

8.7. Foreign material deposits characterisation according to the particle algorithm

In 27 cases (12.9 %), foreign material deposits with uniform morphology were observed. The foreign material deposits were characterised with the aid of the particle algorithm. They were grey-black, Oil Red O-negative particle conglomerates (diameter: around 70–140 μm) consisting of: 1) oval and rectangular, very light micro-particles with dark edges (diameter = 10 μm); 2) Adjacent black micro-particles (diameter $\geq 1 \mu\text{m}$); 3) oval, exclusively peripheral Oil Red O-positive vacuoles (diameter = 50 μm) corresponding to partially dissolved materials. The oval and rectangular particles that are light in colour with dark edges presented an intense birefringence under polarised light. The adjacent black-coloured micro-particles presented a weak homogenous birefringence under polarised light (Fig. 5a, b), and the oval, peripheral Oil Red O-positive vacuoles showed no polarisation birefringence (Fig. 5b). In all 27 cases with foreign material deposits, there were no perifocal histocyte, macrophage infiltrates or foreign body giant cell reactions in the area of the particle deposits. The particle deposits were found in the fibrous, fibroblast- and fibrocyte-rich tissue and showed no or minimal perifocal lymphocyte inflammation infiltration (Fig. 5c).

8.8. Sinus mucous membrane

In 8 cases, sinus mucous membrane was found. This represented 6.5 % of the upper jaw samples (n = 122). They showed inflammation changes consistent with chronic sinusitis. An increased content of eosinophils indicating a so-called allergic sinusitis was not observed Table 1.

9. Discussion

9.1. Apical inflammation processes and bony participation

Apical lesions arise from an infection of the dental pulp. Epithelium remains at the root can proliferate due to the bacterial inflammatory stimulus and result in a radicular cyst. The samples came from 51 dental clinics in three federal German states and were processed in a period of 11 months at a pathology centre that is active across Germany. No samples were rejected. The study can therefore be considered to be

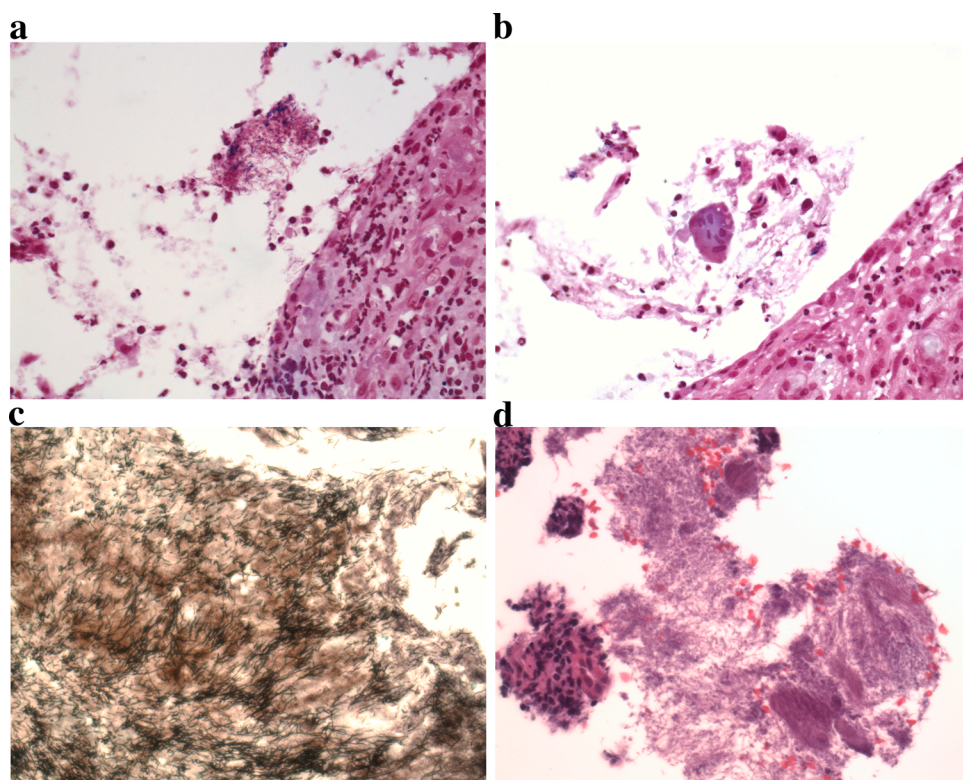


Fig. 3. Histopathological bacteria detection. A, large extracytoplasmic aggregate with various forms of bacteria (cocci, bacilli and vibrio) with varied Gram staining (Gram-positive, Gram-indeterminate and Gram-negative). B, an intracytoplasmic, small aggregate in a macrophage in the form of Gram-positive cocci, and bacilli. C, Grocott-positive extracytoplasmic *Actinomyces israelii* colonies. D, HE-positive extracytoplasmic aggregates of various bacterial forms (cocci, bacilli and vibrio). The bacteria were observable in variably large bacterial-extracytoplasmic aggregates (A and D), intracytoplasmic in small aggregates (B) and in large colonies in case of *Actinomyces israelii* (C). (Original magnification: A and B around 200x, C and D around 400 x).

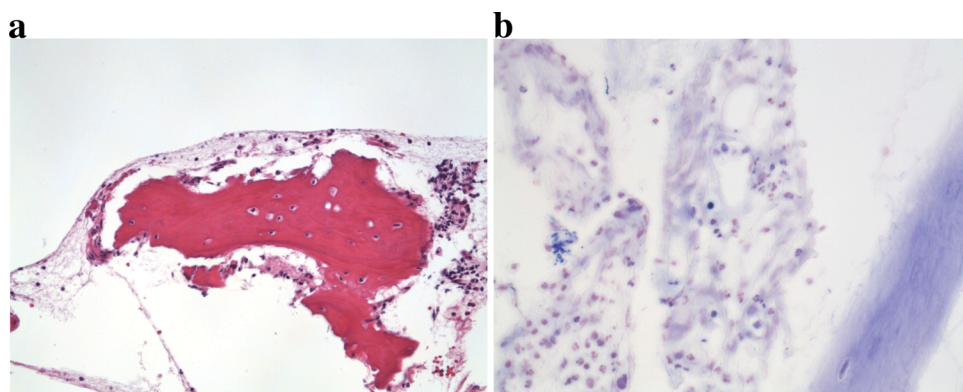


Fig. 4. Osteitis and close spatial relation of bacteria.

A, Granulocyte-rich osteitis of a bone fragment (HOES: indication of acute osteitis) with layered fibrin precipitates, neutrophils, irregular bone surface and individual optically empty osteocyte lacunae indicating osteocyte apoptosis (HE staining; original magnification around 200 x). B, Direct spatial relation of intracellular Gram-positive bacteria localised in macrophages and also extracellular bacteria to bone tissue (in bottom right of image). (Gram-staining; original magnification around 400 x).

randomised in terms of its selection of patients.

The incidence of cysts was described here as 27.2%. The incidence of apical cysts described to date has varied strongly between 6 and 55% [11,15]. The large variance was ascribed to differences in the patient selection and sample sections. In this study, two microtome sections were investigated based on histopathological routine diagnostics, and only fully developed cyst epithelium was considered. The incidence of foreign bodies in the apical lesions was described here as 12.9%. For comparison, incidences between 0.4 and 31% have been described, and have been ascribed to sealers, gutta-percha or other root filling materials [27–30]. The observed foreign material deposits presented no bounding by macrophages or by foreign body giant cells and were non-reactively embedded in fibrous tissue (Fig. 5c). Similar observations have already been described by Love and Firth 2009 [29]. Overall, this observation was interpreted as indicating a high biocompatibility of the endodontic filling materials even in the case of extraradicular locations.

Furthermore, bone fragments were found in 141 (67.1%) samples. To date, bone fragments have only been mentioned or described by Stockdale in 8 of 1018 cases [4,28]. In some studies on the incidence of

apical lesions, bone fragments were not described. [11,15,27,29]. A possible explanation was a long demineralisation period of up to several weeks resulting in bone fragments dissolving. For example, in Ricucci et al. the demineralisation period was 3–4 weeks, and in Ramachandran et al. 1996 “several weeks”. Lamgeland, Stockdale, Chen, and Love do not provide any information in this regard [11,15,27,29]. In comparison, the demineralisation period in this study was at most 3 h.

Differences in the number and relation of acute and chronic inflammation have already been described numerous times [11,27,29,31]. However, what was lacking was a standardised diagnostic assessment according to a defined score for the histopathological diagnosis. For the quantification of the inflammation a semi-quantification (low grade versus high grade) was selected, as it appeared meaningful and was feasible for routine diagnostic assessments. This allowed inflammatory radicular lesions to be categorised into 4 groups according to their histopathological inflammatory infiltration pattern. 81 cases were assigned to Type 1 (acute inflammation = low, chronic inflammation = low), 79 cases into Type 2 (acute inflammation = low, chronic inflammation = high), 46 cases into Type 3 (acute inflammation = high,

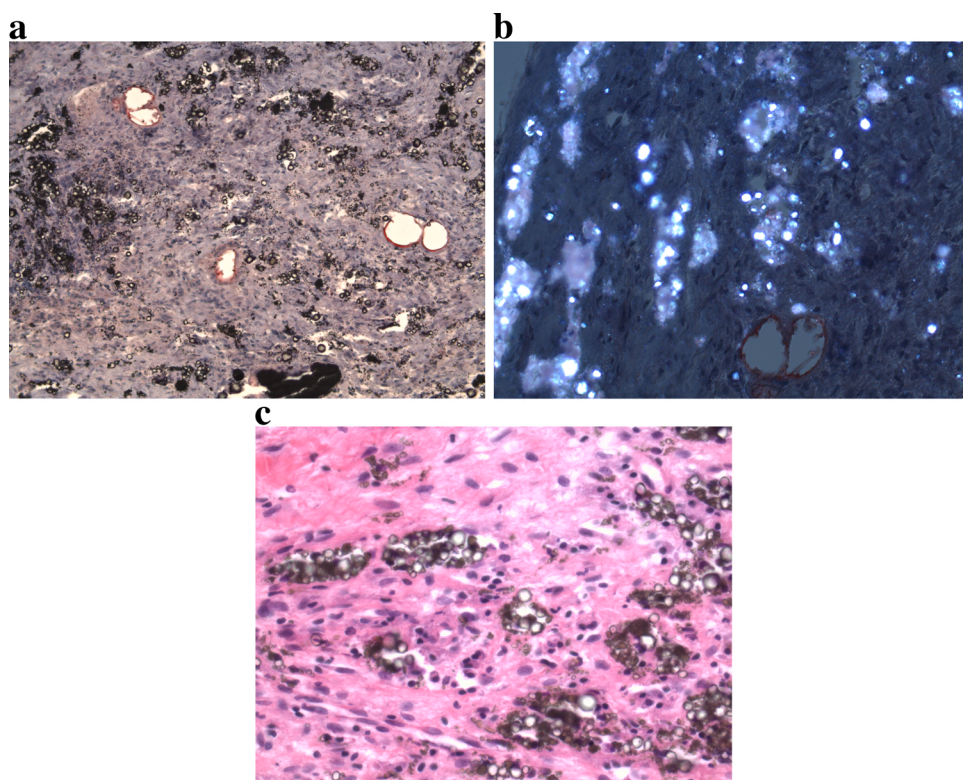


Fig. 5. Foreign material deposits and inflammatory reactions.

A, Aggregated extracellular foreign material deposits as grey-black, Oil Red O-negative particle conglomerates (diameter: around 70 to 140 μm) consisting of: 1) oval and rectangular, very light micro-particles with dark edges (diameter = 10 μm); 2) Adjacent black micro-particles (diameter \geq 1 μm) and 3) oval, exclusively peripheral Oil Red O-positive vacuoles (diameter = 50 μm). **B**, the oval and rectangular particles that are light in colour with dark edges presented an intense birefringence under polarised light. The adjacent black micro-particles presented a weak, homogenous birefringence under polarised light, while the oval, peripheral Oil Red O-positive vacuoles showed no polarisation birefringence (Oil Red O stain and polarised light analysis, original magnification around 400 x). **C**, the particle deposits were evident in the fibrous, fibroblast- and fibrocyte-rich tissue and showed no or minimal perifocal lymphocyte inflammatory reactions with infiltration of individual plasma cells (HE staining, original magnification around 400 x).

Table 1
Differences of DAIS Types regarding Incidence, Epithelium, Osteitis and Bacteria.

	DAIS 1 (acute inflammation = low, chronic inflammation = low)	DAIS 2 (acute inflammation = low, chronic inflammation = high)	DAIS 3 (acute inflammation = high, chronic inflammation = low)	DAIS 4 (acute inflammation = high, chronic inflammation = high)
Incidence ¹	38.6 %	37.6 %	21.9 %	1.9 %
Epithelium ¹	27.2 %	15.2 %	8.7 %	50 %
Osteitis ²	16.1 %	29.8 %	77.8 %	100 %
Bacteria ³	30 %	25 %	55 %	100 %

1) based on 210 samples; 2) based on 141 samples containing bone tissue; 3) based on 64 samples.

chronic inflammation = low) and 4 cases into Type 4 (acute inflammation = high, chronic inflammation = high). Regarding the age and the sample size, no statistically significant relations to the DAIS types could be observed. This allowed the conclusion to be drawn that the DAIS types did not represent different stages of development related to the size of the cyst or the age of the patient. However, as only 4 cases were assigned to DAIS Type 4, statistical testing was difficult.

Epithelium was found in DAIS 1 in 27.2 %, in DAIS 2 in 15.2 %, in DAIS 3 in 8.7 % and in DAIS 4 in 50 % of the samples ($p = .016$ Fisher's exact test). When limiting the observation to DAIS types 1, 2 and 3, it can be stated that either a low acute or a low chronic inflammation favoured cyst epithelium, while cyst epithelium was rarer in the case of a high acute or high chronic inflammation. This conforms to the existing literature [10,32]. However, when a high acute and high chronic inflammation was present in DAIS 4, this resulted in the greatest observed frequency of cyst epithelium. DAIS Type 4 had to be considered separately from the other types with regard to this property.

Bone fragments were analysed with HOES for indications of a bacterial infection. In this study, only bone fragments that were embedded

in the inflammatory infiltrate were investigated. For this reason, there was no participation of the bone marrow and it made sense to report on bacterial osteitis instead of osteomyelitis. As bone fragments were pre-conditions for the diagnosis of bacterial osteitis, only the 141 samples with bone fragments were used to draw conclusions about bacterial osteitis. Osteitis was found in DAIS 1 in 16.1 %, in DAIS 2 in 29.8 %, in DAIS 3 in 77.8 % and in DAIS 4 in 100 % of the samples ($p < .001$, Fisher's exact test). We could therefore conclude that for DAIS 3 and DAIS 4 a bacterial osteitis was highly likely and that both high acute infiltration and high chronic infiltration favoured osteitis. But the acute cell infiltrate was by far the greater factor. This was confirmed by the comparison of DAIS 2 (chronic high-grade; acute low-grade) with 29.8 % osteitis and DAIS 3 (chronic low-grade; acute high-grade) with 77.8 % osteitis. All conclusions regarding DAIS Type 4 were merely indicative, as this group only contained 1 sample with bone fragments. A supporting microbial confirmation of the osteitis diagnosis was not subsequently possible with histological samples.

To investigate the distribution of bacteria within the DAIS types, Gram, Giemsa and Grocott staining were used to investigate 20 samples each from DAIS 1, 2, 3 as well as 4 samples from DAIS 4 for bacteria. Bacteria were found in DAIS 1 in 30 %, in DAIS 2 in 25 %, in DAIS 3 in 55 % and in DAIS 4 in 100 % of the investigated samples ($p = .013$ Fisher's exact test). In all, bacteria were therefore found in 26 of 64 cases (40.6 %). For comparison, Ricucci et al. 2006 found bacteria in 18 of 50 cases (36 %) in apical lesions in necrotic areas with Brown and Brenn staining [15]. The greatest share of bacteria was found in DAIS Type 3 and 4. In comparison, the share in DAIS Types 1 and 2 was significantly lower. This confirmed previous conclusions that a bacterial infection was highly likely in DAIS Types 3 and 4. Histopathologically, DAIS 3 and 4 were characterised by a dense, confluent infiltration pattern of neutrophils (acute high-grade). This infiltration pattern corresponded to the histopathological bacterial infection criteria of joint infections. Illigner et al. found a 93.3 % correlation between histopathological indications of a bacterial infection and its microbiological confirmation [33]. The histopathological properties of the infiltrate, the confirmation of

bacteria, and the assessment of the bone particles according to HOES indicated that for DAIS 3 and DAIS 4 a bacterial infection in the periapical, fibrous tissue was highly likely.

To confirm bacterial colonisation of bone fragments, 12 cases with granulocyte-rich bacterial osteitis were analysed under the microscope. In 4 of the 12 cases bacteria in segmented neutrophils and macrophages as well as extracellular bacteria aggregates (Fig. 4b) could be located in the vicinity of bone tissue fragments. The low proportion of bacteria on bone particles compared to the surrounding tissue was mainly explained by the fact that the samples mostly only contained few bone fragments. The existing surface area for detection was therefore significantly smaller. The preparation of the samples, the sample sectioning and the resolution limits of an optical microscope were limiting factors for the detection of bacteria. In addition, it was assumed that in some cases the removal procedure had dissolved and thus disrupted the continuity of fibrous and bony tissue. But as a spatial relation between inflammation infiltrate in bone tissue and bacteria could be found in some of the cases, these data suggested a bacterially induced osteomyelitis.

As a next step the DAIS should be implemented into clinical situations. As DAIS 3 and 4 indicate bone destruction with bacterial infection, antibiotic therapy after the extraction of the tooth might be of use to support wound healing and bone regeneration. Regarding implantation into those extraction sites the DAIS could be of use to determine time between extraction of the tooth and implantation as well as the risk for further infections. As residual infection at extraction sites due to previous apical periodontitis is considered to be a factor for peri-implantitis [34,35]. Extraction sites with DAIS 1 and 2 should be considered low risk whereas extraction sites with DAIS 3 and 4 should be considered high risk.

A general restriction was the fact that the infection diagnosis used here was a histopathological and therefore descriptive diagnostic tool and that direct pathogen detection, for instance through molecular PCR or MALDI techniques or microbiological methods with germ cell specification or resistance testing, could not be applied. However, the significance of these detection methods was greatly reduced by the specific localisation, with its likelihood of contamination through the oral flora; this in turn increased the significance of the histopathological, direct bacterial detection.

10. Conclusion

DAIS provides the possibility to determine periapical inflammations quantitatively and qualitatively, as well as to determine their causes, using a simple standard staining. DAIS 1–4 show statistically significant differences regarding epithelium, bacterial osteitis and bacterial infiltration. The score could be of clinical use to help determine wound healing, and the risk for further infections.

11. Recommendation for the DAIS reporting

For reasons of practicability and simplified representation of the histopathological routine diagnosis in dental medicine, the following method is suggested:

DAIS classification (DAIS 1–4)

Assessment of the bone tissue with HOES

Statement on epithelial components

If particles detected: descriptive characterisation of the particulate material

Funding

The authors received no specific funding for this work.

Declaration of Competing Interest

The authors report no declarations of interest.

References

- [1] P.N. Ramachandran Nair, Light and electron microscopic studies of root canal flora and periapical lesions, *J. Endod.* 13 (1) (1987) 29–39. S.
- [2] U. Sjogren, B. Hagglund, G. Sundqvist, K. Wing, Factors affecting the long-term results of endodontic treatment, *J. Endod.* 16 (10) (1990) 498–504, [https://doi.org/10.1016/S0099-2399\(07\)80180-4](https://doi.org/10.1016/S0099-2399(07)80180-4). S.
- [3] Thomasvon Arx, Apical surgery: a review of current techniques and outcome, *Saudi Dent. J.* 23 (1) (2011) 9–15. S.
- [4] Kaare Langeland, Farmington Conn, Robert M. Block, Richmond Va, Grossman, I. Louis, A histopathologic and histobacteriologic study of 35 periapical endodontic surgical specimens, *J. Endod.* 3 (1) (1977) 8–23. S.
- [5] Manuel Weber, Jutta Ries, Maiké Büttner-Herold, Carol-Immanuel Geppert, Marco Kesting, Falk Wehrhan, Differences in inflammation and bone resorption between apical granulomas, radicular cysts, and dentigerous cysts, *J. Endod.* 45 (10) (2019) 1200–1208. S.
- [6] S. Liapatas, M. Nakou, D. Rontogianni, Inflammatory infiltrate of chronic periradicular lesions: an immunohistochemical study, *Int. Endod. J.* 36 (7) (2003) 464–471. S.
- [7] I.J. Marton, C. Kiss, Characterization of inflammatory cell infiltrate in dental periapical lesions, *Int. Endod. J.* 26 (2) (1993) 131–136. S.
- [8] Aleksandra Lukic, Vesna Danilovic, Renata Petrovic, Comparative immunohistochemical and quantitative analysis of inflammatory cells in symptomatic and asymptomatic chronic periapical lesions, *Vojnosanit. Pregl.* 65 (6) (2008) 435–440, <https://doi.org/10.2298/vsp0806435l>. S.
- [9] Z. Gao, I.C. Mackenzie, B.R. Rittman, A.K. Korszun, D.M. Williams, A.T. Cruchley, Immunocytochemical examination of immune cells in periapical granulomata and odontogenic cysts, *J. Oral Pathol.* 17 (2) (1988) 84–90. S.
- [10] Louis M. Lin, T.-J. Huang, George, A. Rosenberg, Paul, Proliferation of epithelial cell rests, formation of apical cysts, and regression of apical cysts after periapical wound healing, *J. Endod.* 33 (8) (2007) 908–916. S.
- [11] P.N. Ramachandran Nair, Gion Pajarola, Schroeder, E. Hubert, Types and incidence of human periapical lesions obtained with extracted teeth, *Oral Surg. Oral Med. Oral Pathol. Oral Radiol. Endod.* 81 (1) (1996) 93–102. S.
- [12] S. Colic, M. Jurisic, V. Jurisic, Pathophysiological mechanism of the developing radicular cyst of the jaw, *Acta Chir. Jugosl.* 55 (1) (2008) 87–92, <https://doi.org/10.2298/aci0801087c>. S.
- [13] S. Meghji, W. Qureshi, B. Henderson, M. Harris, The role of endotoxin and cytokines in the pathogenesis of odontogenic cysts, *Arch. Oral Biol.* 41 (6) (1996) 523–531. S.
- [14] Daniela Scalas, Janira Roana, Paolo Boffano, Narcisa Mandras, Cesare Gallesio, Mario Amasio, et al., Bacteriological findings in radicular cyst and keratocystic odontogenic tumour fluids from asymptomatic patients, *Arch. Oral Biol.* 58 (11) (2013) 1578–1583. S.
- [15] Domenico Ricucci, Elizeu A. Pascon, Thomas R.Pitt Ford, Kaare Langeland, Epithelium and bacteria in periapical lesions, *Oral Surg. Oral Med. Oral Pathol. Oral Radiol. Endod.* 101 (2) (2006) 239–249. S.
- [16] B.A. Fisher, R. Jonsson, T. Daniels, M. Bombardieri, R.M. Brown, P. Morgan, S. Bombardieri, W.F. Ng, A.G. Tzioufas, C. Vitali, P. Shirlaw, E. Haacke, S. Costa, H. Bootsma, V. Devauchelle-Pensec, T.R. Radstake, X. Mariette, A. Richards, R. Stack, S.J. Bowman, F. Barone, Sjögren's histopathology workshop group (appendix) from ESSENTIAL (EULAR Sjögren's syndrome study group). Standardisation of labial salivary gland histopathology in clinical trials in primary Sjögren's syndrome, *Ann. Rheum. Dis.* 76 (7 July) (2017) 1161–1168, <https://doi.org/10.1136/annrheumdis-2016-210448>. Epub 2016 Dec 13. PMID:27965259.
- [17] V. Krenn, L. Morawietz, G.R. Burmester, R.W. Kinne, U. Mueller-Ladner, B. Muller, Haul T.Synovitis score: discrimination between chronic low-grade and high-grade synovitis, *Histopathology* 49 (4 October) (2006) 358–364. PMID:16978198.
- [18] L. Morawietz, R. Classen, J.H. Schröder, et al., Proposal for a histopathological consensus classification of the periprosthetic interface membrane, *J. Clin. Pathol.* 59 (2006) 591–597.
- [19] V. Krenn, L. Morawietz, G. Perino, H. Kienapfel, R. Ascherl, G.J. Hassenpflug, M. Thomsen, P. Thomas, M. Huber, D. Kendoff, D. Baumhoer, M.G. Krukemeyer, S. Natu, F. Boettner, J. Zustin, B. Köbel, W. Rütther, J.P. Kretzer, A. Tiemann, A. Trampuz, L. Frommelt, R. Tichilow, S. Söder, S. Müller, J. Parvizi, U. Illgner, T. Gehrke, Revised histopathological consensus classification of joint implant related pathology, *Pathol. Res. Pract.* 210 (12 December) (2014) 779–786, <https://doi.org/10.1016/j.prp.2014.09.017>. Epub 2014 Oct 17. Review. PMID:25454771.
- [20] A. Tiemann, G.O. Hofmann, M.G. Krukemeyer, V. Krenn, Langwald S. Histopathological Osteomyelitis Evaluation Score (HOES) - an innovative approach to histopathological diagnostics and scoring of osteomyelitis, *GMS Interdiscip. Plast. Reconstr. Surg. DGPW* 3 (October) (2014), 20Doc08. doi: 10.3205/ipsr000049. eCollection 2014. PMID:26504719.
- [21] B. Köbel, S. Wienert, J. Dimitriadis, D. Kendoff, T. Gehrke, M. Huber, L. Frommelt, A. Tiemann, K. Saeger, Krenn V.CD15 focus score for diagnostics of periprosthetic joint infections: neutrophilic granulocytes quantification mode and the development of morphometric software (CD15 quantifier), *Z. Rheumatol.* 74 (7 September) (2015) 622–630, <https://doi.org/10.1007/s00393-015-1571-8>. German. PMID: 25869074.
- [22] V. Krenn, G. Perino, W. Rütther, et al., 15 Jahre histopathologischer synovialitis-score, *Z. Rheumatol.* 76 (2017) 539–546, <https://doi.org/10.1007/s00393-017-0308-2>.
- [23] G. Perino, S. Sunitsch, M. Huber, D. Ramirez, J. Gallo, J. Vaculova, S. Natu, J. P. Kretzer, S. Müller, P. Thomas, M. Thomsen, M.G. Krukemeyer, H. Resch, T. Hügler, W. Waldstein, F. Boettner, T. Gehrke, S. Sesselmann, W. Rütther, Z. Xia, E. Purdue, Krenn V.Diagnostic guidelines for the histological particle algorithm in

- the periprosthetic neo-synovial tissue, *BMC Clin. Pathol.* (18 August) (2018) 7, <https://doi.org/10.1186/s12907-018-0074-3>, 25eCollection 2018.PMID: 30158837.
- [24] A. Najm, B. Le Goff, C. Orr, R. Thurlings, J.D. Cañete, F. Humby, S. Alivernini, A. Manzo, S.A. Just, V.C. Romão, V. Krenn, U. Müller-Ladner, O. Addimanda, S. W. Tas, M. Stoenoiu, L. Meric de Bellefon, P. Durez, V. Strand, M.D. Wechalekar, J. E. Fonseca, B. Lauwerys, U. Fearon, D.J. Veale, EULAR Synovitis Study Group and OMERACT Synovial Tissue Special Interest Group. Standardisation of synovial biopsy analyses in rheumatic diseases: a consensus of the EULAR Synovitis and OMERACT Synovial Tissue Biopsy Groups, *Arthritis Res. Ther.* 20 (1 December) (2018) 265, <https://doi.org/10.1186/s13075-018-1762-1>, 3Erratum in: *Arthritis Res Ther.* 2018 Dec 19;20(1):282.PMID:30509322.
- [25] Tatiana Anatolievna Stupina, Anatoliy Sergeevich Sudnitsyn, Koushik Narayan Subramanyam, Nikolai Sergeevich Migalkin, Anastasia Yrievna Kirsanova, Sagar Umerjekar, Applicability of histopathological osteomyelitis evaluation score (HOES) in chronic osteomyelitis of the foot - A feasibility study, *Foot Ankle Surg.* (2019).
- [26] V. Krenn, P. Thomas, M. Thomsen, J.P. Kretzer, S. Usbeck, L. Scheuber, G. Perino, W. Rütter, R. v. Welsler, F. Hopf, Huber M.HIstopathological particle algorithm. Particle identification in the synovia and the SLIM], *Z. Rheumatol.* 73 (7 September) (2014) 639–649, <https://doi.org/10.1007/s00393-013-1315-6>. German.PMID:24821089.
- [27] Jeng-Huey Chen, Chih-Huang Tseng, Wen-Chen Wang, Ching-Yi Chen, Fu-Hsiung Chuang, Yuk-Kwan Chen, Clinicopathological analysis of 232 radicular cysts of the jawbone in a population of southern Taiwanese patients, *Kaohsiung J. Med. Sci.* 34 (4) (2018) 249–254. S.
- [28] C.R. Stockdale, N.P. Chandler, The nature of the periapical lesion—a review of 1108 cases, *J. Dent.* 16 (3) (1988) 123–129. S.
- [29] R.M. Love, N. Firth, Histopathological profile of surgically removed persistent periapical radiolucent lesions of endodontic origin, *Int. Endod. J.* 42 (3) (2009) 198–202. S.
- [30] H.S. Koppang, R. Koppang, S.O. Stolen, Identification of common foreign material in postendodontic granulomas and cysts, *J. Dent. Assoc. S. Afr.* 47 (5) (1992) 210–216. S.
- [31] Domenico Ricucci, Louis M. Lin, Larz S.W. Spångberg, Wound healing of apical tissues after root canal therapy: a long-term clinical, radiographic, and histopathologic observation study, *Oral Surg. Oral Med. Oral Pathol. Oral Radiol. Endodontology.* 108 (4) (2009) 609–621. S.
- [32] P.N.R. Nair, Pathogenesis of apical periodontitis and the causes of endodontic failures, *Crit. Rev. Oral Biol. Med.* 15 (6) (2004) 348–381. S.
- [33] U. Illgner, V. Krenn, N. Osada, L. Bause, Histopathology and microbiology of joint infections: extension of diagnostic safety in patients with chronic polyarthritis, *Z. Rheumatol.* 72 (7 September) (2013) 709–713, <https://doi.org/10.1007/s00393-013-1173-2>.
- [34] Z. Esfahrood, M. Rezaei; Kadkhodazadeh, R. Amid, A.R. Rohn, Is the periapical lesion a risk for periimplantitis? (a review), *J. Dent. (Tehran)* 9 (2) (2012) 162–173. S.
- [35] G. Marshall, L. Canullo, R.M. Logan, G. Rossi-Fedele, Histopathological and microbiological findings associated with retrograde peri-implantitis of extraradicular endodontic origin: a systematic and critical review, *Int. J. Oral Maxillofac. Surg.* 48 (11) (2019) 1475–1484. S.